6th International Conference on Multiphase Flow,
ICMF 2007, Leipzig, Germany, July 9 – 13, 2007

Scale effects on gas transport by hydraulic jumps in inclined pipes; comparison based on head loss and breakdown rate

C.L. Lubbers*,** and F.H.L.R. Clemens**

* WL | Delft Hydraulics, P.O. Box 177, 2600 MH Delft, the Netherlands. (E-mail: Christof.Lubbers@wldelft.nl) (primary contact)
** Delft University of Technology, Faculty of Civil Engineering and Geosciences, Section of Sanitary Engineering, P.O. Box 5048, 2600 GA Delft, the Netherlands. (E-mail: f.h.l.r.clemens@citg.tudelft.nl)

Keywords: scale effects, experimental research, hydraulic jumps, pressure mains, head loss removal of gas pockets

Abstract

In The Netherlands, the waste water pressure mains suffer from capacity reduction due to gas accumulated at high points in the system. A 3-year research was carried out to investigate the gas transport phenomena in a downward sloping pipe as well as the head loss that gas accumulation creates when the flow velocity remains lower than a critical value. Moreover, the breakdown rate of a gas pocket by the gas transport capacity of the flow is studied. Three experimental setups have been designed and built to investigate these issues. The majority of the experiments were carried out for a pipe diameter of 220 mm. To investigate the validity of the results for other diameters, one geometry of the downward sloping section of 10° is scaled to a diameter of 110 mm and 500 mm. The results of this study show that, when taking the scale into account, the results of the 220 mm and 500 mm diameter yield similar results, whereas the results from the 110 mm experiments deviate. This paper focusses on the experiments carried out on the slope of 10°, for a diameter of 110 mm, 220 mm and 500 mm.

Introduction

Sewer systems have two main functions: collecting and transporting wastewater and storm water out of urban areas. The collection and transport of wastewater is initiated by the urge to maintain a high level of public hygiene. Combined with a high quality of drinking water this results in an important reduction of the occurrence of infectious diseases. Though other methods exist to remove wastewater and storm water out of urban areas the application of underground systems (sewer systems) is by far the most commonly applied.
In the Netherlands in most of urban areas, the classic concept of urban drainage, a gravity system is applied. Four systems can be distinguished:

- The combined sewer system.
- The improved combined sewer system.
- The separate system.
- The improved separate system.

Especially in The Netherlands, the Wastewater Treatment Plants (WWTP) are located outside the urban areas. The sewerage from the sewer systems is conveyed to the WWTP's by pressurised mains. The length of these pressure mains range between hundreds of meters and tens of kilometres. Pumping stations convey the water through these mains often in a intermittent manner. The intermittent character of the flow depends on the sewer supply and the type of operation of the pumps. In this paper, the discussion is limited to these sewer pressure mains.
Most of the wastewater pressure mains have been designed to convey only water, rather than a gas-water mixture. As sewerage contains gas, the flow velocity must be large enough to convey this gas through the entire pressure main. The flow capacity is reduced when the water flow rate is not sufficiently large to carry gas, which will lead to an accumulation of gas, mostly at high points in the system. In the case that a gas pocket is present in a downward sloping pipe section, energy is lost which results in a capacity reduction of the pump system.
In hydraulic transients the volume of the gas pockets change, which causes sudden acceleration and deceleration of the flow, giving rise to unpredictable pressure values.
Gas pockets may come into movement after exceeding a critical threshold value, which may lead to gas blow-outs or blow-backs, risking material damage to the pipe.

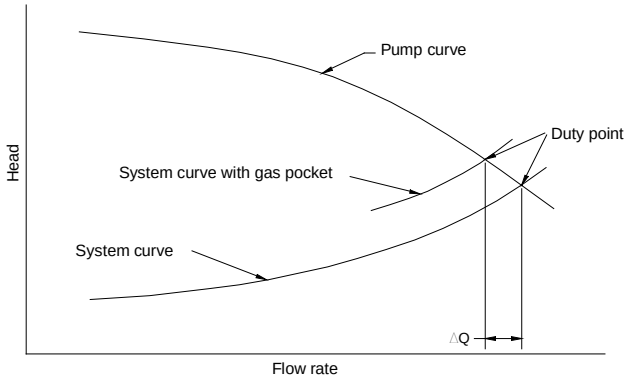

Figure 1. QH curve of pump and system with additional head loss caused by a gas pocket.

Figure 1 presents the pump and system curve, which is a relation between the head and flow capacity delivered by the

pump. The intersection of the two curves defines the duty point of the pump. If an additional head loss is created due to a gas pocket, the system curve rises leading to a duty point with a smaller flow rate. The additional head loss due to the gas pocket could be so large that the flow rate drops to zero. If the design capacity is not reached, the public will observe this by CSO spills, water in the street and less direct by a higher tax due to larger energy costs. Burrows and Qiu (1996) investigated and proved that small gas pockets in sewer pressure mains were the cause of repeated pipe failure. Gas pockets cause a potential unpredictability of a pipeline's performance and integrity.

Nomenclature

a	Coefficients
c	Coefficient
g	Gravitational constant (ms^{-1})
n	Scale factor (-)
q	Flow rate (m^3s^{-1})
p	Pressure (Nm^{-2})
t	Time (s)
v	Velocity (ms^{-1})
z	Level (m)
A	Area (m^2)
D	Pipe diameter (m)
H	Energy head (m)
L	Pipe length (m)

Greek letters

α	Slope angle (°)
ε	Energy dissipation rate per unit mass (m^2s^{-3})
ρ	Density (kgm^{-3})
η	Viscosity (Pa·s)
λ	Hydraulic resistance coefficient (-)
σ	Standard deviation
ξ	Friction factor (-)

Subsripts

1	Upstream
2	Downstream
110	D = 110 mm
220	D = 220 mm
500	D = 500 mm
dry	dry
max	maximum
rise	rise
G	gas
L	liquid

Experimental Facility

General layout D = 220 mm

The experiments were conducted in a dedicated facility for research on air/gas pockets that are located at the transition from horizontal to inclined pipes. The facility (Figure 2) was specially designed to inject a controlled and monitored airflow rate into the liquid phase. From a constant head reservoir, a pump circulates water through the experimental facility. The test section consists of a horizontal section, and at the air injection point a downward sloping section is followed by a horizontal section.

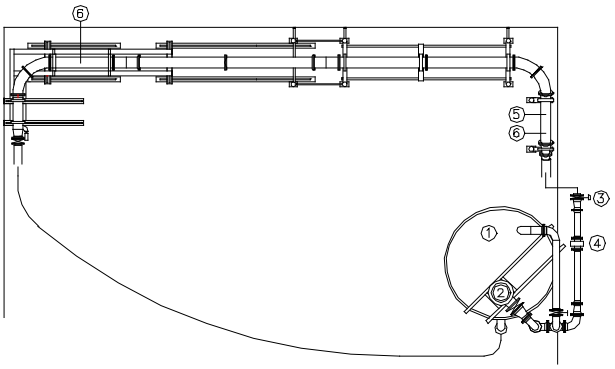

Figure 2. op view of the experimental setup. 1: reservoir, 2: pump, 3:control valve, 4: electromagnetic flowmeter, 5: air injection point, 6: upstream and downstream pressure transmitters.

Figure 2 and Figure 3 show the general layout of the test section that represents a high point in a system. The test section is made of transparent material (Perspex) with an inner diameter D = 220 mm. Flexible hoses connect the test section to the reservoir and pump. The test section consists of a horizontal pipe section of 2m (L = 9D), a downward sloping pipe of 6 m (L = 27D) followed by a horizontal pipe section of 2 m (L = 9D). While the downstream end of the test section has a fixed elevation (ground level), the upstream end of the test section can be varied to obtain the desired inclination angle α. The bends have one sharp angle.

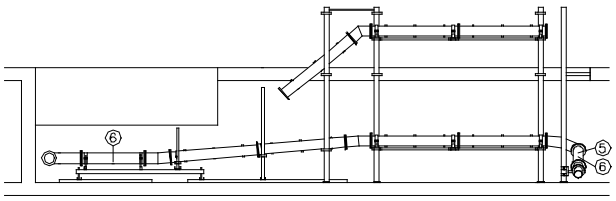

Figure 3. Side view of the experimental setup

An overview of the experimental setup is presented in Figure 2. The frequency driven pump (2) that is located in a high reservoir (1) circulates the water through the test section. Although the speed of the pump can be varied, the water flow rate is controlled by a control PC that receives a signal from the electromagnetic flow meter (4) and sends a signal to the flow control valve (3).
A flow control valve (3), in combination with an electromagnetic flow meter (4) and PC, adjusts the flow rate to its set value.
The water/air mixture returns to the reservoir over a weir in order to strip as much air as possible from the water. The injection of air into the system results in a head increase in the pump, causing the flow rate to drop. The flow control allows a constant flow rate during head changes.

General layout D = 110 mm

The influence of the diameter was studied by comparing the results of head loss and breakdown rate in three identical test sections layout. The reference test section with D =220 mm was scaled to 110 mm and 500 mm. The reference geometry with α = 10º, L = 6m and D = 220 mm was scaled with scale factor n = 110/220. Figure 4 displays a photograph of the 110 mm test section.

Figure 4. Layout of the 110 mm test section, α = 10º and *L* = 27D.

General layout D = 500 mm

The influence of the diameter was studied by comparing the results of the head loss and breakdown rate in three identical test section layouts. The reference test section with *D* =220 mm was scaled to 110 mm and 500 mm. The reference geometry with α = 10º, *L* = 6m and *D* = 220 mm was scaled with a scale factor *n* = 500/220.

Instrumentation and flow control

The range and uncertainty of the instruments are listed in Table 1.

Pressure transmitter

For the 220 mm setup, two pressure transmitters were located in the test section mounted in the bottom of the pipe to avoid air disturbing the measurement. One was located in the approaching pipe section upstream of the upstream horizontal part (6). The other one was downstream of the test section in the horizontal pipe (6).

For the 110 mm setup, instead of 2 absolute pressure transmitters upstream and downstream of the test section, one absolute pressure transmitter upstream and one pressure differential pressure transmitter over the test section was used. The location of the tappings was identical to the 220 mm test section.

For the 500 mm setup, the location of the downstream tapping was identical to the 220 mm test section, but the upstream pressure transmitter was located in the vertical standpipe.

Water flow rate

The flow rate was measured by an electromagnetic flow meter (EMF).

Air flow rate

The air flow meter measures mass flow rate instead of volume flow rate. The output gives 'nl/min', i.e., a volumetric flow rate at normal conditions (101325 Pa and 0 °C). As the pressure in the test section varied, it was not of interest to control the flow rate for normal condition values. The air flow rate was controlled volumetrically with reference to the upstream pressure and reservoir temperature.

Temperature

The temperature was measured with a PT100 pressure transmitter, located in the reservoir. The signal was used to monitor possible heating of the water by the pump.

Air flow rate control

Air was supplied by the standard 6-bar pressurised air-infrastructure in the building. A combined mass flow meter and flow control (5) maintains the airflow to its set point.

Water level

To assess the water depth, the circumference of the outside diameter was measured by means of readings from a flexible ruler taped around the pipe.

Table 1. List of instrumentation

Instrument	Measuring range	Uncertainty (based on 2σ)
electromagnetic flow meter DN 125 (EMF)	0 – 100 l/s	< 0.25 % of full scale
Gas flowmeter	1-50 nl/min	< 0.50 % of full scale
2 absolute pressure transmitters	0 – 3 bar	< 0.1 % of full scale
4 pressure differential transmitters	1.20 mbar 2-5 bar	< 0.1 % of full scale
Temperature transmitter	3 – 100 °C	< 0.1 °C

Energy loss measurements

Assess stationary situation

The measurements were carried out under stationary conditions. The time scale at which the phenomena took place ranged from tenths of seconds to hours. Especially the flow conditions close to the critical flow velocity and low air discharge rates (q_G < 5 l/min) show a long (on the order of an hour) adaptation period to reach the equilibrium state after a flow rate change. Initially, the air discharged from the tail of the gas pocket may be very close but not equal to the gas supply. The gas pocket is growing but the grow rate was not visible with the eye and can erroneously be taken as stationary. The upstream and downstream pressures are sampled and the pressure difference is plotted during testing on a large time scale. Figure 5 shows an example of a record of a growing gas pocket. Only if the pressure differential line was at a constant level, was a measurement taken.

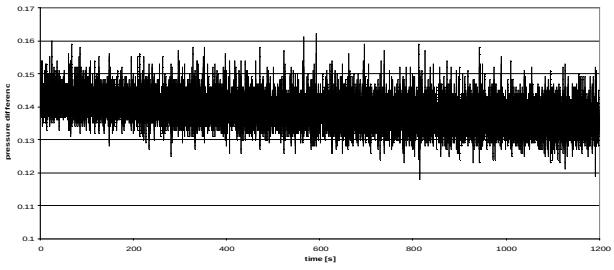

Figure 5. The end of an adaptation period from one flow condition to another.

Data acquisition

If the stationary condition was achieved, the water and air flow rate, the upstream and downstream pressure and the water temperature signals were recorded. All signals have been recorded for 30 seconds at a sample rate of 100 Hz, yielding 3000 samples per measurement. The sample rate was sufficiently high to represent the 'spikes' in the pressure difference signal

Breakdown rate measurements

Breakdown rate measurements were carried out to study the rate at which a gas pocket is removed. The measurements were carried out for several water flow rates and inclination angles. The initial condition for breakdown rate measurements is the stationary situation with the maximum gas flow rate (q_G = 25 l/min) and a water flow rate of choice. The measurements start by closing the valve of the gas supply.

The inherent gas discharge rate of the hydraulic jump was determined by supplying a larger air flow rate towards the high point than the water flow rate would naturally be able to transport. A stationary condition is reached when the gas pocket is larger than would normally occur. If a stationary situation has been established, the air supply is shut off. From that moment on, the gas discharge is larger than the supply and the gas pocket volume will consequently decrease. The decrease in the gas pocket is determined using two pressure transmitters. The breakdown rate is quantified by calculating the shift in the location of the hydraulic jump per unit of time. The breakdown rate is calculated in this manner for several values of α in order to compare the efficiency of the hydraulic jump for different inclination angles. As soon as the stationary situation is achieved, the air supply is shut off and the water and air flow rate, the upstream and downstream pressure and the water temperature signals are recorded.

Data acquisition

The water and gas flow rate, the upstream and downstream pressure and the water temperature as a function of time were recorded. All signals are recorded until the gas pocket disappears, with a maximum period of 5 hours at a sample rate of 1 Hz.

All signals were recorded at a sample rate of 1 Hz until the whole air pocket vanished or a period of 5 hours passed. If the gas pocket had not been removed after this time span, the breakdown rate of the gas pocket is regarded as very slow i.e., ~ 0 l/min.

The sample rate is proven to be sufficiently high to follow the change in the pressure difference signal well.

Method of analysis

Energy loss

The energy loss produced by the gas volume was calculated based on the energy balance between pressure transmitters 1 and 2.

The energy losses between those points were caused by:

- friction losses along the pipe wall
- deceleration losses at the two bends
- losses due to the gas pocket.

The Bernoulli energy balance reads:

$$z_1 + \frac{p_1}{\rho g} + \frac{v_1^2}{2g} = z_2 + \frac{p_2}{\rho g} + \frac{v_2^2}{2g} + \left(\sum_i \xi_{loc,i} + \lambda \right) \frac{L}{D} \frac{v_2^2}{2g} + \Delta H_{gas}$$

The level difference ($z_1 - z_2$) was determined by measuring the pressure at point 1 and 2 at no-flow condition. This value is corrected for the offset obtained from the calibration of the pressure transmitters.

The total head loss due to wall and internal friction and deceleration is measured for several water flow rates without gas supply. A second order polynomial is fitted through the measuring points and used in further calculations for the dynamic energy loss. Hence:

$$\Delta H_{dyn} = \left(\xi_{loc} + \lambda \frac{L}{D} \right) \frac{v_2^2}{2g} = a_0 + a_1 v_2 + a_2 v_2^2$$

The values of a were determined for every geometry. The uncertainty in the dynamic head loss was calculated using the general equation for error accumulation:

$$\Delta H_{gas} = z_1 - z_2 + \frac{p_1 - p_2}{\rho g} - \left(a_0 + a_1 v_2 + a_2 v_2^2 \right)$$

At the 110 mm test section, the differential pressure transmitter measures directly the pressure loss over the test section. Information about H_{stat} is therefore not required.

The values of ΔH_{gas} are presented as a function of the dimensionless velocity:

$$v' = \frac{v}{\sqrt{gD}} = \frac{q_L}{\frac{1}{4}\pi g \sqrt{D} D^2}$$

Breakdown rate

The breakdown rate of the gas pocket by the discharge of small bubbles from the hydraulic jump is influenced by many parameters, such as inclination angle, water velocity, and/or water depth at the foot of the hydraulic jump. The breakdown rate is determined for a number of combination water flow rates and inclination angles. Prior to the measurement, an initial gas volume is injected into the pipe. The size of the volume depends on the water flow rate. The breakdown rate is calculated from the pressure difference over the test section.

The pressure signal fluctuates in time and a moving average filter is applied prior to calculating the time derivative of the pressure difference. The breakdown rate is defined as:

$$\frac{1}{\rho g} \frac{d\Delta p}{dt} = \frac{1}{\rho g} \frac{\left(\Delta p_{t_2} - \Delta p_{t_1} \right)}{t_2 - t_1}$$

where Δp is the pressure difference in Pascal at time t, which is expressed in hours, ρ is the density of water and g is the gravitational acceleration.

During the measurement the water flow rate is kept constant by the flow rate control. This implies that the control PC is gradually closed as the gas pocket diminishes in size, resulting in a smaller head loss caused by the gas pocket. The control valve maintains a constant total system head loss, thus keeping the flow rate constant. The closing of the control valve, which is located upstream of the test section, causes a pressure decrease in the test section, causing the gas volume to expand.

The pressure in a real system changes due to changes in the resistance and head loss. If the gas pocket decreases in size, or actually height, the head loss over the gas pocket will decrease and the flow rate of the pump will increase. The increased flow rate, in its turn, has an increasing effect on the

pressure due to greater dynamic resistance in the system. In total, the pressure in the system will decrease and the gas pocket will expand. So, a part of the breakdown rate of the gas pocket is compensated by expansion due to the pressure decrease.
Although the head loss depends on the height of the gas pocket, it does not linearly depend on volume change. The shape of the volume plays a large role. The water depth in the pipe significantly influences the length. The ratio between the value upstream of the bend and the volume downstream determines the total change of the of the gas pocket height. The water depth is almost completely determined by the water flow rate.
The relative volume change increases as the water depth increases. If the water flow rate changes at constant pressure, A_{dry1} changes to A_{dry2} and L_1 to L_2 at constant volume as follows:

$$V_{gas} = \int_{l=0}^{L_1} A_{dry1} dl = \int_{l=0}^{L_2} A_{dry2} dl$$

In practice, the pressure in the systems changes with flow rate changes. It is assumed that the ideal gas law, which states that the product of the pressure and volume is constant if the temperature of the gas does not change during the process, is valid. Constant temperature may be assumed if the volume change is slow. On points in time t_1 and t_2 the following is valid:

$$p_1 V_1 = p_2 V_2 = p_2 \left(V_1 + \Delta V_{12} \right)$$

The volume change from V_1 to V_2 reads:

$$\Delta V_{12} = V_1 \frac{\left(p_1 - p_2 \right)}{p_2} = V_1 \frac{\Delta p_{12}}{p_2}$$

Depending on the ratio of the volume upstream and downstream of the bend, the length of the gas pocket in the inclined pipe and thus the head loss increase will change. The water level will not change due to pressure changes. This implies that all volume change is projected in the inclined pipe. The head loss change reads:

$$\Delta H = \frac{\Delta V_{12}}{A_{dry}} \sin \alpha$$

Due to the volume change, the expression for the breakdown rate needs to be corrected. If the volume increases due to a pressure decrease, the gas volume actually removed is larger than calculated from the pressure difference measurements. The following correction is applied:

$$\frac{1}{\rho g} \cdot \frac{\left(\Delta p_2 - \Delta p_1 \right)}{t_2 - t_1} - \frac{V_1 \Delta p_{12}}{p_2 A_{dry} \left(t_2 - t_1 \right)} \sin \alpha$$

The breakdown rate is determined as a function of the height of the gas volume. The vertical height is thus a measure for head loss. The head loss reads:

$$H_{airpocket} = z_1 + \frac{p_1}{\rho g} - z_2 - \frac{p_2}{\rho g}$$

In order to compare flow rates with those for other pipe diameters, a dimensionless velocity is defined as follows:

$$v' = \frac{v}{\sqrt{gD}}$$

where v is the mean velocity for the fully filled pipe and D is the diameter of the pipe.

Results and Discussion

Head loss

In this section, the head loss is presented in two absolute and one relative way. The *total head loss* ΔH_{total} is the sum of the dynamic head loss and head drop caused by the presence of a gas pocket measured between the upstream and downstream pressure transmitters. The *head loss* ΔH_{gas} caused by the gas pocket is the total head loss measured minus the measured dynamic head loss for pure water without gas presence. The dynamic head loss was determined by measuring the pressure difference over the test section and determine the hydraulic resistance coefficient λ according to the definition of the dynamic head loss over a pipe section L.
Both head losses mentioned have the dimension of length expressed in meters. The third description is the *dimensionless head loss* $\Delta H'$ defined as:

$$\Delta H' = \frac{\Delta H_{gas}}{L \sin \alpha - \left(D - y_{\min} \right)}$$

Figure 6 shows the total head loss measured for α = 10° as a function of the water flow velocity for several gas flow rates ranging from q_G = 1 l/min to 25 l/min. The star markers present the measurements of the dynamic head loss between the two pressure transmitters for q_G = 0. A polynomial was fitted through these points and was used to calculate the difference between the total head loss and the dynamic head loss defined by the polynomial. For a given q_G, the general trend of the total head loss showed a decrease with an increasing value of v. Furthermore, at a given v, the head loss increased with increasing values of q_G.

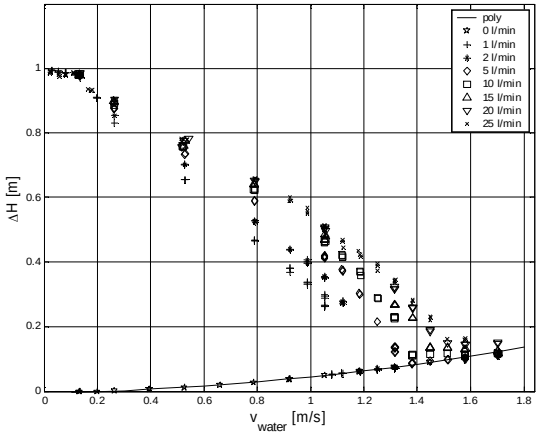

Figure 6. Head loss at different water and gas flow rates

with α = 10º and L = 6 m.

The maximum head loss occurring for v = 0 m/s has the value of the vertical level difference of the pipe minus the height of the air layer at the location where the flow is critical. Figure 6 shows a maximum head loss of 0.98 m which corresponds well to 0.96, which is the defined maximum head loss at q_L = 5 l/s. This maximum head loss was defined as follows:

$$\Delta H_{\max} = L\sin\alpha - \left(D - y_{\min}\right)$$

This equation presents the vertical distance between the locations where the flow changed from a sub-critical to a supercritical flow in the upstream horizontal part and the inside top of the pipe of the downstream horizontal part. The decrease of the head loss as a function of the water flow rate was not the same for every gas flow rate. While the head loss decreased smoothly for the larger gas flow rates, it decreased rapidly around v = 1.1 m/s for small gas rates (as shown in Figure 6). For q_G = 1 and 2 l/min the head drops almost instantly to zero.

Figure 7 shows ΔH_{gas}, i.e. the total head loss minus the polynomial fit of value ΔH_{dyn}. The critical velocity for which no additional head loss caused by the gas supply occurs (threshold value of 0.5 D) is v_c = 1.1 m/s for q_G = 1 l/min and 1.5 m/s for q_G = 25 l./min.

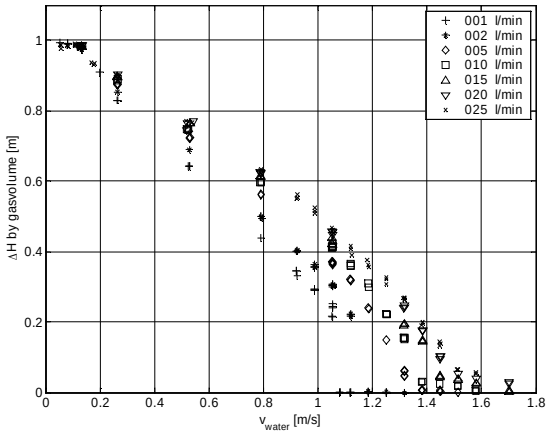

Figure 7. The head loss caused by the gas flow rate for a = 10º and L = 6m

Most experiments were carried out at D = 220 mm. One geometry, namely for α = 10º, L = 6 m and D = 220 mm was taken as the reference to study the influence of the diameter on the head loss. This test section was geometrically scaled to D = 110 mm and D = 500 mm. The values for q_L and q_G are Froude scaled according to:

$$q_1 = \left(\frac{D_1}{D_2}\right)^{2.5} q_2$$

This implies an equal gas/liquid flow rate ratio at the beginning of the test section. The validity of the results for D = 220 mm for other diameters was tested with these two setups. The results are plotted for the three geometries for q_G equivalent to 1 and 2 l/min for D = 220 mm.

Some measurements for D = 110 mm and v' < 0.3 produced a hydraulic jump that was pushed into the downstream horizontal section. These measurements are left out of the graphs.

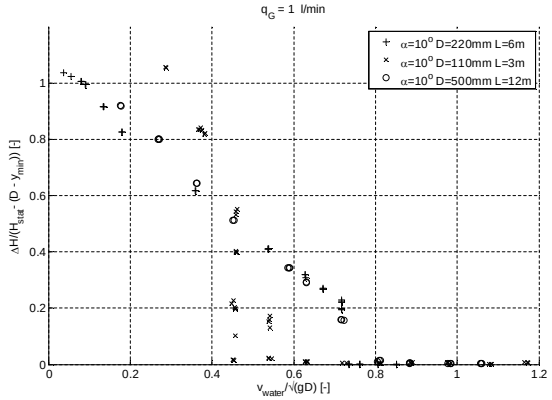

Figure 8. Influence of the D on the head loss for q_G = 1 l/min (scaled with D = 220 mm as reference)

Figure 8 shows many interesting results. First, the presentation of the head loss by $\Delta H'$ and v' seems to work out well. Both for the D = 220mm and 500mm test sections, $\Delta H'$ coincides over a large range of v'. It can be concluded that only small differences of $\Delta H'$ are present between identical geometries with D = 220mm and 500mm. This implies that the results of the head loss measurements for D = 220 mm can be extrapolated to larger diameters without any significant diameter/scale effects. Scaling from D = 110 mm to D = 220 and 500 mm does not yield realistic results. The results for D = 110 mm show a larger head loss for v' < 0.4. This could be explained by a relatively larger buoyancy / drag ratio in this range for D = 110 mm compared to D = 220 mm. The ratio of bubble rise velocity (v_{rise} = 0.20 to 0.25 m/s for both diameters) to flow velocity is given in Table 2. For v' = 0 - 0.20, $v_{rise} > v$. This agrees with the observation that the head loss is equal to or greater than the level difference of the horizontal pipe sections, i.e. the water flow is not able to remove the gas bubbles.

Table 2. Ratio of rise and flow velocity between diameters

v'	v_{110}	v_{rise}/v_{110}	v_{220}	v_{rise}/v_{220}
0.1	0.10	2.41	0.15	1.70
0.2	0.21	1.20	0.29	0.85
0.3	0.32	0.80	0.44	0.57
0.4	0.42	0.60	0.59	0.43

This results in a relatively larger up-flow of gas and therefore a higher head loss. For v' > 0.4, the head loss is smaller for D = 110 mm than for D = 220 and 500 mm. At v' = 0.4, the head loss very steeply decreases to smaller values. The gas bubbles apparently experience relatively more drag and are transported more easily than bubbles with larger diameters.

In order to find the maximum bubble diameter, one assumes in the common approach adopted locally isotropic turbulence and break-up to be affected by energy containing eddies of size l_e. The dynamic pressure experienced by the bubble, assuming the maximum diameter d_{max} to be equal to the size of the eddy, becomes:

$$\Delta p = const \cdot \rho_L \left(d_{\max}\varepsilon\right)^{2/3}$$

This dynamic thrust pressure will be opposed both by the viscosity of the bubble and by the interfacial tension. Gas bubbles are less viscous than the continuous phase thus surface tension will be the only break-up opposing force. The force around the circumference will be $\pi d\sigma$, acting across an area $\pi d^2/4$ leads to a pressure holding the bubble together of $4\sigma/d$. When the pressure of the dynamic thrust fluctuations of the turbulent flow field is less than $4\sigma/d$, the bubble will be stable. The maximum diameter for a bubble in the turbulent flow field can be calculated from:

$$\rho_L \left(d_{\max}\varepsilon\right)^{2/3} = c' \cdot \frac{4\sigma}{d_{\max}}$$

where c' is a constant to be determined from experiments. Rearranging, the expression for the maximum diameter becomes:

$$d_{\max} = k\left(\frac{\sigma}{\rho_L}\right)^{0.6} \varepsilon^{-0.4}$$

According to Hinze (1955) $k = 0.725$ based on measurements by Clay (1940) of drop sizes in liquid flowing between two coaxial cylinders, the inner one of which rotated. For turbulent pipe flow the maximum size of the dispersed fluid particles then can be calculated by substituting $\varepsilon = 2f_m u_m^3/D$, where f_m is the friction factor, D is the pipe diameter and u_m the mixture velocity. This then gives:

$$d_{\max} = 0.725\left(\frac{\sigma}{\rho_L}\right)^{0.6}\left(2 f_m \frac{u_m^3}{D}\right)^{-0.4}$$

Figure 9 shows the trend of the maximum bubble diameter d_{max} as a function of the dimensionless velocity v' according to this equation.

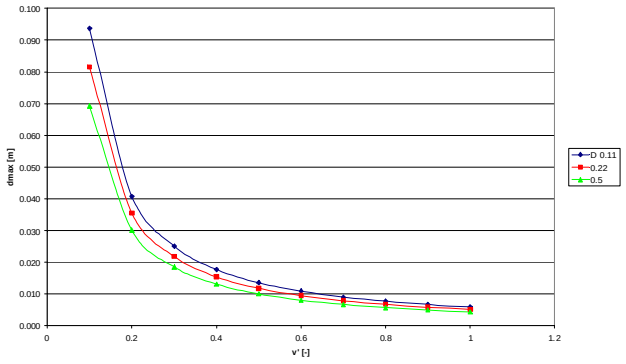

Figure 9. Maximum bubble size as function of v'

For a given v' the bubbles are larger for a smaller D. This means that fewer bubbles per volume are present in the case with smaller D, or the bubble density is less. For a given value of v', the flow velocity v is smaller and therefore the bubble diameter d is larger for decreasing values of D. This implies that the transport of gas bubbles, due to a larger buoyancy-to-drag ratio, is mitigated for decreasing values of D for all v'. Figure 8 shows, however, that that line of reasoning is only observed for $v' < 0.4$. For $v' > 0.4$, other mechanisms play a role that even may enhance gas transport.

Figure 10 displays the dimensionless head loss for the three geometries (D = 110, 220 and 500 mm) for q_G = 2 l/min (scaled to D = 220 mm). The graph of $\Delta H'$ for D = 110 mm shows a steep decrease starting with a relatively large head loss that changes to a relatively small head loss having a transition point at $v' = 0.5$.

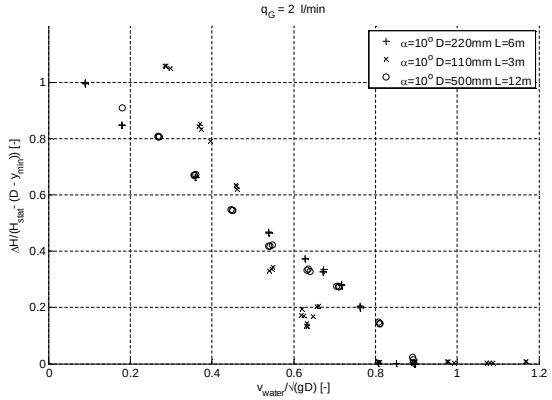

Figure 10. Influence of the diameter on the head loss for q_G = 2 l/min equivalent gas flow rate

Breakdown rate

If gas is present in pressurised pipelines, it tends to accumulate at high points. The water flow transports the gas present in the pipe to this point and, depending on the flow velocity and amount of gas accumulated; the air is transported further through the downward sloping pipe.

At moderate water velocities, *all* gas transport is carried out by small bubbles rather than by large gas pocket transport. The mechanism that creates the favourable condition of small bubbles in the fluid is the hydraulic jump located in the inclined pipe. The hydraulic jump, however, is not always present. The criterion that must be met is the occurrence of the critical flow at the bend. This is only possible if sufficient gas has accumulated at the high point. If the gas supply is larger than the gas discharge, the water level can drop to the minimum specific energy value that corresponds to the water flow rate.

Experiments were carried out to study the breakdown rate of a gas pocket at several geometrical and flowing conditions. A large number of α, L, D and q_L were tested. The experiment started with the maximum gas pocket length that could be obtained in the test section for the involved test condition with q_G = 25 l/min. The moment the gas supply was cut off to zero, the measurement started.

Figure 11 shows the breakdown rate as a function of the height of the gas pocket. It clearly shows that for a given hydraulic jump location or head loss, the breakdown rate increases for increasing values of v'. It also shows that for a given supply of gas to the pipe system, the resulting head loss is larger for smaller v'.

The shape of the graph is divided into two parts. First, the 'linear' part. Here, the hydraulic jump is fully developed and

the breakdown rate decreases slowly in time by varying the Froude number upstream of the hydraulic jump and the length between the end of the hydraulic jump and the downstream bend. The figures show that for small v' (0.18 and 0.36), the linear part is dominant. This can be explained by the length of the hydraulic jump that increases with increasing values of v'. For increasing values of v', the linear part decreases and the curved part increases. For $v' = 0.18$, it is observed that the head loss caused by the gas pocket decreased from 80 cm to 40 cm in 4 hours' time. So, it took 4 hours to remove 40 cm of head loss. For $v' = 0.36$ and 0.54, the gas transport capacity increased, but the removal process in a pipe with $L = 6$ m, still takes hours. For $v' = 0.72$ and 0.81, the gas transport capacity has increased significantly. At flow rates smaller than a 'critical' value ($q_L < 30$ l/s), the removal of gas will take hours and the gas pocket will not be removed completely, thus a gas pocket will remain.

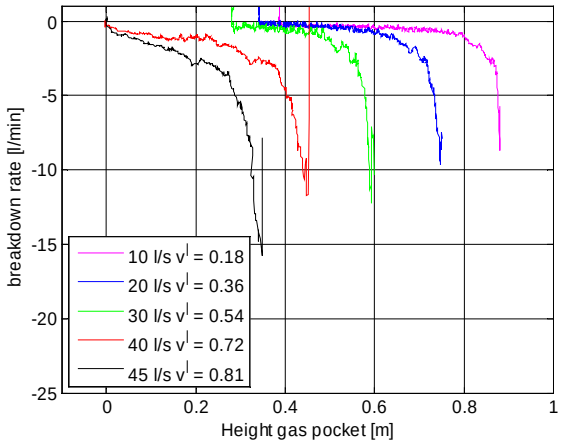

Figure 11. Breakdown rate [l/min] as function of head loss for α =10°

The influence of the diameter on the breakdown process was investigated for two other diameters: a smaller diameter of 110 mm and a larger one of 500 mm.
The results of the breakdown rate for $D = 110$ and $D = 500$ mm Froude scaled to $D = 220$ mm according:

$$q_G|_{D_2} = q_G|_{D_1} \left(\frac{D_2}{D_1} \right)^{2.5}$$

Figure 12 presents the breakdown rates scaled to $D = 220$ mm for α = 10°, and for $D = 110$ mm, 220 mm and 500 mm for $v' = 0.36$. The results for $v' = 0.18$, 0.54 and 0.72 show that Froude scaling of the breakdown rate gives similar results for $D = 220$ mm and 500 mm, and that for $D = 110$ mm, the breakdown rate is relatively larger. The breakdown rate is expressed as the height of the gas pocket divided by D to take the diameter into account when relating it to the location of the hydraulic jump. An exception is seen in the results for $v' = 0.18$, where the breakdown rate for $D = 500$ mm is very small to negligible.

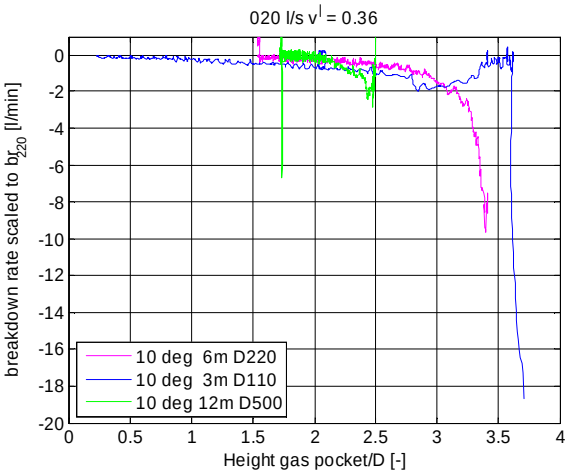

Figure 12. Breakdown rate for $v' = 0.36$ scaled to $D = 220$ mm as function of the height of the gas pocket divided by the diameter for α = 10 ° for $D = 110$ mm, 220 mm and 500 mm.

The results for $v' = 0.72$ show that scaled values are similar for the $D = 220$ mm and 500 mm pipes. It can be concluded that the breakdown rate can be scaled according to Froude for diameters in the larger range ($D = 220$mm to 500mm). For the smaller diameter this seems not to be the case. The results for $D = 110$ mm show a larger scaled breakdown rate than for $D = 220$ mm and 500 mm. For the head loss measurements (Figure 8 and Figure 10), similar trends have been observed for $v' > 0.4$, where the head loss results for $D = 110$ mm were much lower than for $D = 220$ mm and 500 mm.

Conclusions

Head loss

The influence of the diameter is obtained by experiments on a pipe section with α = 10º and diameters $D = 110$ mm, 220 mm and 500 mm. Based on these experiments, it can be concluded that the head loss results scaled to one diameter is about equal for $D = 220$ mm and 500 mm. The results from the $D = 110$ mm experiments deviate from the $D = 220$ mm and 500 mm results.

Breakdown rate

The influence of the diameter is obtained by experiments on a pipe section with α = 10º and diameters $D = 110$ mm, 220 mm and 500 mm. Based on these experiments, it can be concluded that the breakdown rate results scaled to one diameter is about equal for $D = 220$ mm and 500 mm. The results from the $D = 110$ mm experiments are higher than for the $D = 220$ mm and 500 mm results.

Acknowledgements

The research is funded by: Foundations RIONED and STOWA, the Waterboards of Aquafin, Brabantse Delta, Delfland, DWR, Fryslân, Municipality of The Hague, Hollandse Eilanden en Waarden, Hollands Noorderkwartier, Reest en Wieden, Rivierenland, Veluwe, Zuiderzeeland and the Engineering/consultancy companies DHV and Grontmij.

References

Clay (1940)

Kent, J.C. The entrainment of Air by Water Flowing in Circular Conduits with downgrade Slopes. Thesis presented to the University of California, at Berkeley, Calif., in 1952.
Hinze (1955)
Lubbers, C.L and Clemens, F.H.L.R (2005) Air and gas pockets in sewerage pressure mains. IWA journal Water Science and Technology, issue 3, volume 52.
Lubbers, C.L and Clemens, F.H.L.R (2006) Breakdown of air pockets in downwardly inclined sewerage pressure mains. IWA journal Water Science and Technology, issue 11-12, volume 54.p233-240
Lubbers, C.L. (2003). Capwat: Resultaten van inventarisatie, voortgangsrapportage-02 (Results of the inventory study, part of the Capwat project) H4230.10 Delft Hydraulics.
Walski, T.M. (1994). Hydraulics of corrosive gas pockets in force mains. Water Environment Research, Volume 66, Number 6.
Wisner, P.E. (1975). Removal of air from water lines by hydraulic means, Proceedings of the American Society of Civil Engineers, Journal of the Hydraulics Division, Vol. 83, No. HY2, February, 1975.